Available online at www.sciencedirect.com
ScienceDirect
Journal of Solid State Chemistry 179 (2006) 2805–2808
Journal of Solid State Chemistry
www.elsevier.com/locate/jssc

Anomalous charge transport in CeB_6 ☆

M.I. Ignatov[a,b,*], A.V. Bogach[a,b], S.V. Demishev[a,b], V.V. Glushkov[a,b], A.V. Levchenko[c], Yu.B. Paderno[c,✠], N.Yu. Shitsevalova[c], N.E. Sluchanko[a]

[a] A.M.Prokhorov General Physics Institute of RAS, 38, Vavilov street, Moscow 119991, Russia
[b] Moscow Institute of Physics and Technology, 9, Institutskii per., Dolgoprudny, Moscow region 141700, Russia
[c] Institute for Problems of Materials Science, UA-252680 Kiev, Ukraine

Received 30 August 2005; received in revised form 15 November 2005; accepted 10 January 2006
Available online 9 February 2006

Abstract

The comprehensive study of conductivity σ, Hall coefficient R_H and Seebeck coefficient S has been carried out on high-quality single crystals of CeB_6 in a wide range of temperatures 1.8–300 K. An anomalous behavior of all transport characteristics (σ, R_H, S) was found for the first time in the vicinity of $T^* \approx 80$ K. The strong decrease of conductivity σ as well as the unusual asymptotic behavior of Seebeck coefficient $S(T) \sim -\ln T$ observed below T^* allowed us to conclude in favor of crossover between different regimes of charge transport in CeB_6. The pronounced change of Hall mobility μ_H, which diminishes from the maximum value of 20 cm^2/(V s) at T^* to the values of ~6 cm^2/(V s) at $T \sim 10$ K, seems to be attributed to the strong enhancement of charge carriers scattering due to fast spin fluctuations on Ce-sites. The low-temperature anomalies of the charge transport characteristics are compared with the predictions of the Kondo-lattice model.

Keywords: Kondo lattice; Charge transport

1. Introduction

It is generally believed that the cerium hexaboride (CeB_6) is an archetypal example of a dense Kondo system [1,2]. This compound crystallizes in the CaB_6-type structure that can be considered as a combination of two simple cubic lattices arranged from Ce-ions and B_6-octahedrons correspondingly and bound covalently to each other. The splitting Δ of the Ce^{3+} $^2F_{5/2}$ state in the cubic crystalline field $\Delta = E(\Gamma_7) - E(\Gamma_8) \approx 530$ K [3] (see the inset in Fig. 1) exceeds considerably the Kondo temperature $T_K \approx 1$–2 K as estimated by different experimental methods (see, e.g., [4]). According to the conclusion [5] one of the most important feature that gives rise to the anomalies of transport and thermodynamic characteristics in this analogue of monovalent metal with strong electron correlations is the coincidence between the number of itinerant electrons (n_e) and cerium 4*f*-sites (n_{4f})—$n_{4f} \approx n_e$. The appearance of complex magnetic structures and unconventional magnetic $H-T$ phase diagram of CeB_6 at liquid-helium temperatures is commonly associated with the n_{4f} and n_e coincidence, as well as with the competition between the Kondo scattering mechanism of charge carriers and the RKKY interaction of localized magnetic moments (LMM) [5]. In accordance with the result for dense Kondo systems [6], the largest amplitude of the Kondo maximum of resistivity $\rho(T)$ is expected in the range of $n_{4f} \approx n_e$. Indeed, it was reliably established for CeB_6 at $T \leqslant 150$ K (see, e.g., [7,8]) that the resistivity increases noticeably (approximately by a factor of 3) with the temperature decrease. However, the analysis of the experimental dependence $\rho(T)$ and the magnetic component in resistivity $\rho_m(T) = \rho(T) - \rho_{LaB_6}(T)$ [7,8] does not reveal any extended region of the Kondo-like dependence $\rho_m(T) \sim -\ln T$ in CeB_6.

Another problem was noted by the authors of [4] when discussing the transport characteristics of CeB_6. The Hall coefficient in CeB_6 unlike the majority of so-called

☆ Presented at ISBB'05.

*Corresponding author. A.M. Prokhorov General Physics Institute of RAS, 38, Vavilov street, Moscow 119991, Russia. Fax: +7 095 135 8129.
E-mail address: ignatov@lt.gpi.ru (M.I. Ignatov).
✠ Deceased.

0022-4596/$ - see front matter © 2006 Elsevier Inc. All rights reserved.
doi:10.1016/j.jssc.2006.01.016

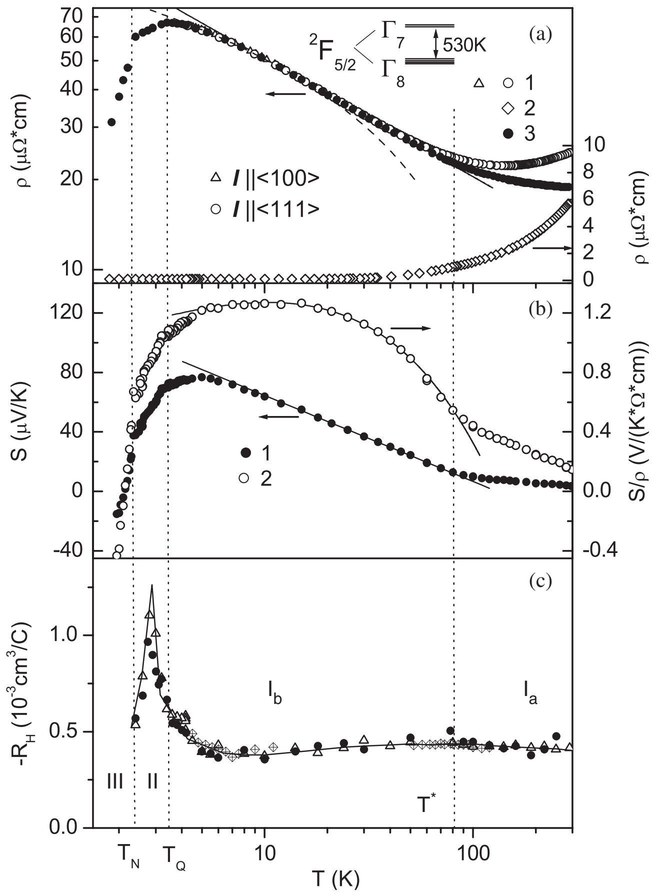

Fig. 1. Temperature dependence of transport coefficients (ρ, R_H, and S): (a) resistivity of (1) CeB_6 for different directions of current passed through the sample, (2) LaB_6, and (3) magnetic contribution $\rho_m(T) = \rho(T) - \rho_{LaB_6}(T)$ (see text). The logarithmic ($\rho \sim -\ln T$) and power ($\rho \sim T^{-1/\eta}$) asymptotics are shown by dotted and solid lines, respectively. The intervals I–III correspond to the paramagnetic (I(a,b)), AFQ(II) and AFM(III) phases in CeB_6. The inset shows the splitting of Ce^{3+} $^2F_{5/2}$ state by crystalline field, (b) temperature dependences of the Seebeck coefficient $S(T)$ and the ratio $S(T)/\rho(T)$ in CeB_6, (c) temperature dependences of the Hall coefficient $R_H(T)$.

Ce-based Kondo lattices is proved to be negative and independent of temperature and magnetic field in the interval of 4.2–300 K within the accuracy of measurements [4,9]. Thus, both the sign of the Hall coefficient and the temperature dependence $R_H(T)$ in CeB_6 contradict to the predictions of the skew-scattering model for $R_H(T, H)$ in dense Kondo systems [10,11]. Another experimental fact that was not adequately interpreted up to now is associated with the behavior of the Seebeck coefficient $S(T)$ in CeB_6. According to calculations in the frameworks of the Kondo-lattice model [12], the broad positive maximum of $S(T)$ should be observed in the vicinity of T_K, whereas the sign of thermopower has to be inversed to negative at $T_{inv} \approx 0.4T_K$. So the observation that the Seebeck coefficient in CeB_6 achieves its maximum value at $T^S_{max} \approx 7 - 10\,K \gg T_K \approx 1\,K$ [5,13] reveals apparent discrepancy between the behavior of $S(T)$ and the theoretical results predicted in the frameworks of the Kondo-lattice model [12].

2. Experiment

To elucidate actual mechanisms responsible for charge transport in CeB_6, precise measurements of the transport coefficients (ρ, R_H, and S) have been carried out with the comparative analysis of these results in wide temperature range. For this purpose high-quality single crystals of CeB_6 were investigated in this work. The synthesis technique of the CeB_6 and the characteristic properties of the samples under investigation are described in [14]. The high precision measurements of $\rho(T)$, $R_H(T)$, and $S(T)$ have been performed in the temperature range of 1.8–300 K using the experimental setups described in [15,16].

3. Results and discussion

Fig. 1a shows the $\rho(T)$ dependencies measured for current applied along different crystallographic directions in CeB_6. Note that no anisotropy of resistivity was detected in this study for current applied along $\langle 100 \rangle$ and $\langle 111 \rangle$ directions. The significant increase of resistivity observed with temperature lowering in the interval $T \leqslant 150\,K$ is followed by falling of $\rho(T)$ below the temperature of magnetic antiferroquadrupole (AFQ) phase transition $T_Q \approx 3.3\,K$. A pronounced kink on the resistivity curve (Fig. 1a) indicates the antiferromagnetic (AFM) phase transition at $T_N \approx 2.3\,K$, which is accompanied by a further decrease in resistivity. It can be clearly seen from the double logarithmic plot of Fig. 1a that the $\rho(T)$ dependence in CeB_6 is well described by the power law $\rho(T) \sim T^{-1/\eta}$ with exponent $1/\eta \approx 0.39 \pm 0.02$. This asymptotic behavior seems to correspond to the regime of weak localization of charge carriers in the entire temperature interval of 7–80 K. Moreover, the value of the critical index $1/\eta \approx 0.39 \pm 0.02$ corresponds with a good accuracy to the value of $1/\eta = 4/11$ obtained in [17]. Note here that the critical index for conductivity $\eta = 11/4$ found for the metallic side of the metal–insulator transition in the framework of the two-parametric scaling approach [17] takes into account the localization effects in combination with strong electron correlations. Besides, the increase in resistivity of CeB_6 within the temperature range 7–80 K cannot be described by the logarithmic Kondo-like dependence $\rho \sim -\ln T$ neither for the initial curve $\rho(T)$ nor for the magnetic contribution to resistivity $\rho_m(T) = \rho(T) - \rho_{LaB_6}(T)$ (see curves 1 and 3 in Fig. 1a).

The analysis of the results of high precision measurements of the Seebeck coefficient in CeB_6 (curve 1 in Fig. 1b) reveals the above-mentioned change in the character of scattering which is also observed on the $S(T)$ curve near $T^* \sim 80\,K$. In this regime of weak localization of charge carriers thermopower drastically increases from the values of $S < 10\,\mu V/K$ at $T > T^* \sim 80\,K$, which are typical for the metallic state, to the values of $S \sim 70–90\,\mu V/K$ near the maximum of the $S(T)$ dependence (Fig. 1b). Besides, in interval I_b thermopower follows to the unusual logarithmic dependence $S(T) \sim -\ln T$ which is accompanied by the power-law asymptotic behavior of resistivity. Taking into account the additive character of a parameter $S/\rho = \Sigma S_i/\rho_i$, which allows for several groups of charge carriers and was earlier applied to other cerium-based intermetallides [18], the discussed change in the regime of charge transport at $T \sim T^* \sim 80$ K can be clearly demonstrated in the representation $S/\rho = f(\ln T)$ (curve 2 in Fig. 1b). As seen from the data of Fig. 1b, the behavior of the transport ratio S/ρ in CeB_6 can be rather well described by the dependence $(S/\rho) \sim T^{1/\eta} \ln T$ in the wide temperature interval $5\,K \leqslant T \leqslant T^* \approx 80$ K. It should be especially pointed out that noticeable deviations of the parameters ρ, S, and S/ρ from the analytical dependencies found in the interval I_b (see Figs. 1a–c) are observed at temperatures below 5 K. These deviations can be evidently interpreted in terms of additional contributions to these transport parameters which appear in the immediate vicinity of magnetic phase transitions at T_Q and T_N in AFQ and AFM phases of CeB_6, respectively.

Further, we shall concentrate on the present results of high precision measurements of the Hall coefficient $R_H(T)$ in CeB_6 (Fig. 1c). The data of Fig. 1c demonstrate clearly that the Hall coefficient of CeB_6 is negative and varies only slightly in the temperature interval of 5–300 K. The pronounced negative anomaly of $R_H(T)$ is observed in the vicinity of the magnetic phase transitions at T_Q and T_N in CeB_6 (Fig. 1c). Such a behavior of $R_H(T)$ in Kondo-lattice compound contradicts to the results of the skew-scattering model calculations [10,11] where the appearance of the positive maximum of Hall effect is expected in vicinity of the Kondo temperature $T_K(CeB_6) \approx 1$–2 K. Another feature of the $R_H(T)$ dependence detected in this study is a very smooth maximum near the temperature of liquid nitrogen (Fig. 1c).

The analysis of parameter $\mu_H(T) = R_H(T)/\rho(T)$ (Fig. 2a) which corresponds to Hall mobility for system with one type of charge carriers, allowed us to conclude evidently about qualitative changes of the scattering of charge carriers in CeB_6 at $T^* \sim 80$ K. When decreasing temperature in the interval $5\,K < T < T^* \sim 80$ K, the parameter $\mu_H(T)$ decreases also approximately by a factor of 3. For Ce-based dense Kondo systems, the situation is just opposite, i.e., $\mu_H(T)$ should rise with decreasing the temperature (see, e.g., [10,15]). Moreover, the temperature dependence of quasielastic-scattering linewidth Γ [19] has been used to estimate the relaxation time $\tau = 2\hbar/\Gamma$ and the effective mass $m_{eff} = e\tau/\mu$ of charge carriers from our data. As shown in the Fig. 2b, the effective mass drastically increases to the maximum value $m_{eff}(5\,K) = 440 m_0$ $(\tau(5\,K) \approx 1.5 \times 10^{-12}$ s) when lowering the temperature in the interval $T = 5-300$ K. Besides, it was found that the effective mass follows to power law $m_{eff} \sim T^{-0.8}$ in the whole temperature interval I_b (Fig. 2b) that does not seem to be explained in terms of Kondo-lattice model [10,15].

The results of precision measurements of charge carrier transport characteristics (Figs. 1, 2) obtained in this study on high-quality single crystals of CeB_6 were compared with

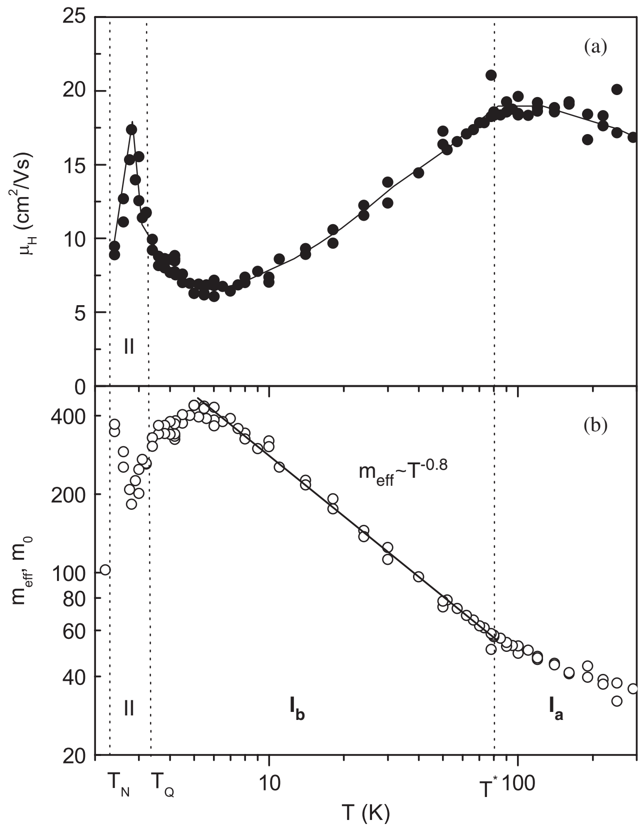

Fig. 2. Temperature dependences of the Hall mobility $\mu_H(T) = R_H(T)/\rho(T)$ in CeB_6 (a) and effective mass m_{eff} in CeB_6 as estimated from Hall mobility μ_H and quasielastic neutron scattering linewidth Γ (b).

the predictions of the approach based on the Kondo-lattice model. The analysis allows us to conclude that the traditional interpretation fails to explain the observed features of the transport characteristics of CeB_6. When discussing alternative approaches for explaining the observed anomalies, it is necessary to take into account the results of the electronic band structure calculations [20]. From this point of view, divalent hexaborides of alkaline- and rare-earth elements are semimetals [20], whereas the transition to trivalent rare-earth ions in the CaB_6-type structure is accompanied by filling of the conduction band with an extremum at the X point in the Brillouin zone. According to the results [20] the conduction band has a significant dispersion and is characterized predominantly by $5d$-states. Besides, the anomalies of transport and thermodynamic characteristics both for doped divalent hexaborides (see, e.g., [21,22]) and for intermediate valence compound SmB_6 [23] have been interpreted in terms of excitonic instability, which is accompanied by a partial or complete dielectrization of electronic structure in these compounds. In such situation, the possibility of any similar scenario should not be ruled out also for CeB_6. According to the approach recently applied to hexaborides $La_xCa_{1-x}B_6$ and $La_xSr_{1-x}B_6$ [23,24], one would expect the development of exciton instability in $5d$-band is expected in case of CeB_6 at $T^* \sim 80$ K. This phase transformation at $T^* \sim 80$ K is also expected to be accompanied with a partial dielectrization of spectrum in the state with charge/spin density waves. Then, at low temperatures, this scenario predicts the transition into a phase of excitonic ferromagnet [24,25], or into a spatially inhomogeneous magnetic multi-domain state with electronic phase separation [21,22]. As a result, the excitonic instability and/or electronic phase separation can induce the appearance of random potential and, consequently, the weak localization asymptotic observed in $\rho(T)$ in this work (Fig. 1a). In our opinion, this kind of interpretation of the low-temperature anomalies in CeB_6 can be strongly supported by the fact that the nature of magnetic phases and the character of phase transitions in this compound with a simple bcc-crystal structure are not fully identified up to now [26]. Therefore, to elucidate the origin of the transition at $T^{*}\sim 80\,K$ and unconventional magnetic ground state of CeB_6, the comprehensive measurements of transport and magnetic properties of CeB_6 at liquid-helium temperatures are of a great interest.

Acknowledgments

This work was supported by the RFBR 04-02-16721 and INTAS 03-51-3036 projects and by the Programs "Strongly Correlated Electrons" of RAS and "Development of Scientific Potential" of MES RF. V.V.G. acknowledges support from Russian Science Support Foundation.

References

[1] N. Sato, S. Kunii, I. Oguro, et al., J. Phys. Soc. Jpn. 53 (1984) 3967.
[2] K. Hanzawa, T. Kasuya, J. Phys. Soc. Jpn. 53 (1984) 1809.
[3] E. Zirngiebl, B. Hillebrands, S. Blumenroder, et al., Phys. Rev. B 30 (1984) 4052.
[4] N. Sato, A. Sumiyama, S. Kunii, et al., J. Phys. Soc. Jpn. 54 (1985) 1923.
[5] C. Marcenat, D. Jaccard, J. Sierro, et al., J. Low Temp. Phys. 78 (1990) 261.
[6] M. Lavagna, C. Lacroix, M. Cyrot, Valence instabilities, in: P. Wachter, H. Boppart (Eds.), North-Holland, Amsterdam, 1982, p. 375.
[7] K. Winzer, W. Felsch, J. Phys. C 6–39 (1978) 838.
[8] N. Sato, S.B. Woods, T. Komatsubara, et al., J. Magn. Magn. Mater. 31–34 (1983) 417.
[9] Y. Onuki, T. Yamazaki, T. Omi, I. Ukon, A. Kobori, T. Komatsubara, J. Phys. Soc. Jpn. 58 (1989) 2126.
[10] P. Coleman, P.W. Anderson, T.V. Ramakrishnan, Phys. Rev. Lett. 55 (1985) 414.
[11] M. Hadzic-Leroux, A. Hamzic, A. Fert, et al., Europhys. Lett. 1 (1986) 579.
[12] K.H. Fischer, Z. Phys. B 76 (1989) 315.
[13] N. Ali, S.B. Woods, J. Appl. Phys. 57 (1985) 3182.
[14] N.B. Brandt, V.V. Moshchalkov, S.N. Pashkevich, et al., Solid State Commun. 56 (1985) 937.
[15] N.E. Sluchanko, A.V. Bogach, V.V. Glushkov, S.V. Demishev, M.I. Ignatov, N.A. Samarin, G.S. Burkhanov, O.D. Chistyakov, JETP 98 (2004) 793.
[16] N.E. Sluchanko, V.V. Glushkov, S.V. Demishev, M.V. Kondrin, N.A. Samarin, V.V. Moshchalkov, V.V. Brazhkin, JETP 86 (1998) 190.
[17] W.L. McMillan, Phys. Rev. B 24 (1981) 2739.
[18] M.I. Ignatov, A.V. Bogach, V.V. Glushkov, S.V. Demishev, G.S. Burkhanov, O.D. Chistyakov, N.A. Samarin, N.E. Sluchanko, Physica B 363 (2005) 252.
[19] S. Horn, F. Steglich, et al., Z. Phys. B: Condens. Matter 42 (1981) 125–134.
[20] S. Massida, A. Continenza, T.M. de Pascale, R. Monnier, Z. Phys. B 102 (1997) 83.
[21] V. Barzykin, L.P. Gor'kov, Phys. Rev. Lett. 84 (2000) 2207.
[22] L. Balents, C.M. Varma, Phys. Rev. Lett. 84 (2000) 1264.
[23] N.E. Sluchanko, V.V. Glushkov, S.V. Demishev, et al., Phys. Rev. B 65 (2002) 064404.
[24] B.A. Volkov, Yu.V. Kopaev, A.I. Rusinov, JETP 41 (1976) 952.
[25] B.A. Volkov, A.I. Rusinov, R.Kh. Timerov, JETP 43 (1976) 589.
[26] O. Zacharko, P. Fischer, A. Schenk, S. Kunii, et al., Phys. Rev. B 68 (2003) 214401.